JOURNAL OF VIROLOGY, May 2011, p. 4470–4479 Vol. 85, No. 9
0022-538X/11/$12.00 doi:10.1128/JVI.01515-10

The C-Terminal nsP1a Protein of Human Astrovirus Is a Phosphoprotein That Interacts with the Viral Polymerase▽

Cristina Fuentes, Susana Guix, Albert Bosch,* and Rosa M. Pintó*

Enteric Virus Laboratory, Department of Microbiology, University of Barcelona, Barcelona, Spain

Received 21 July 2010/Accepted 8 February 2011

Human astrovirus nonstructural C-terminal nsP1a protein (nsP1a/4) colocalizes with the endoplasmic reticulum and viral RNA. It has been suggested that nsP1a/4 protein is involved in the RNA replication process in endoplasmic reticulum-derived intracellular membranes. A hypervariable region (HVR) is contained in the nsP1a/4 protein, and different replicative patterns can be distinguished depending on its variability. In the present work, both the astrovirus RNA-dependent RNA polymerase and four types (IV, V, VI, and XII) of nsP1a/4 proteins have been cloned and expressed in the baculovirus system to analyze their interactions. Different isoforms of each of the nsP1a/4 proteins exist: a nonphosphorylated isoform and different phosphorylated isoforms. While the polymerase accumulates as a monomer, the nsP1a/4 proteins accumulate as oligomers. The oligomerization domain of nsP1a/4-V is mapped between residues 176 and 209. For all studied genotypes, oligomers mainly contain the nonphosphorylated isoform. When RNA polymerase is coexpressed with nsP1a/4 proteins, they interact, likely forming heterodimers. The polymerase binding region has been mapped in the nsP1a/4-V protein between residues 88 and 176. Phosphorylated isoforms of nsP1a/4 type VI show a stronger interactive pattern with the polymerase than the nonphosphorylated isoform. This difference is not observed in genotypes IV and V, suggesting a role of the HVR in modulating the interaction of the nsP1a/4 protein with the polymerase through phosphorylation/dephosphorylation of some critical residues.

Human astroviruses, first described as a cause of infantile gastroenteritis in 1975 (2, 16), are nonenveloped single-stranded positive-sense RNA viruses that belong to the *Astroviridae* family (23), which includes both mammalian and avian viruses. The ~6.8 kb polyadenylated viral genome is composed of three open reading frames (ORFs): 1a, 1b, and 2. ORF2, located at the 3′ end of the genome, encodes the viral capsid protein through a 2.4-kb subgenomic RNA (24), whereas both ORF1a and ORF1b, which contain the conserved motifs for a 3C-like serine protease and an RNA-dependent RNA polymerase, respectively, are translated directly from the genomic viral RNA (11, 15, 17, 18). Upon infection, the nonstructural proteins (nsPs) are translated from the genomic RNA as two large polyproteins, nsP1a and nsP1a/1b, through a (−1) ribosomal frameshifting mechanism (11, 15, 17). The processing of the astrovirus nonstructural polyproteins has not been completely characterized, and some of the reported data are still conflicting. Although there is no confirmation by N-terminal sequencing of the processing products, at least four cleavage sites have been suggested within nsP1a, and it is assumed that both viral and cellular proteases are responsible for the process (4, 5, 14, 21, 30). Thus, nsP1a polyprotein would generate at least four products, which in this work will be named nsP1a/1, nsP1a/2, nsP1a/3 (protease), and nsP1a/4, which could be processed even further. The exact boundaries of these proteins are not well defined. Two cleavage sites yielding the nsP1a/4 have been proposed at positions Gln-567/Thr-568 (14) and Glu-654/Ile-655 (4, 27), which would render products of 40.1 and 30.6 kDa, respectively. With antibodies against a broad region of the nsP1a C terminus, Méndez and colleagues (21) and Willcocks and colleagues (30) reported proteins of 20 kDa and of 34, 20, 6.5, and 5.5 kDa, respectively, but no other cleavage sites were suggested. Previous data from our laboratory with an antibody against a peptide belonging to amino acid positions 778 to 792 of nsP1a revealed proteins of 160 kDa, 75 kDa, 38 to 40 kDa, and 27 to 21 kDa in HAstV-infected CaCo-2 cells (7). The crystal structure of an nsP1a/3-derived protein, whose boundaries are from amino acids 432 to 587, has very recently been resolved (27), suggesting that the cleavage site between nsP1a/3 and nsP1a/4 proteins occurs at Glu-654/Ile-655.

With the exception of nsP1b and nsP1a/3, which encode the RNA-dependent RNA polymerase (RdRp) and the 3C-like serine protease, respectively, the roles of the rest of the nonstructural mature products are mostly unknown. Sequence analysis has predicted four transmembrane domains and a helicase conserved motif close to the nsP1a N-terminal end (1, 11). In the nsP1a C-terminal end, named here the nsP1a/4 protein, several domains have been described: two coiled-coil regions, one coinciding with a death domain (DD), a nuclear localization signal (NLS), a putative viral genome-linked protein (VPg), and a hypervariable region (HVR) (1, 6, 11, 13, 22, 25, 29). Based on the HVR nucleotide genetic variability, 15 different nsP1a/4 protein HVR-derived genotypes (named using Roman numerals) have been established, and a restriction fragment length polymorphism (RFLP) typing method has been developed to consistently distinguish between genotypes (9). In addition, computational analyses of the nsP1a/4 coding region performed in our laboratory revealed the presence of acidic regions and of glutamine- and proline-rich regions, a death domain, and several putative O-glycosylation and phosphorylation sites (6–8). Biological and functional analyses also

* Corresponding author. Mailing address: Department of Microbiology, University of Barcelona, Diagonal 645, 08028 Barcelona, Spain. Phone: (34) 934034620/21. Fax: (34) 934034629. E-mail for A. Bosch: abosch@ub.edu. E-mail for R. M. Pintó: rpinto@ub.edu.

▽ Published ahead of print on 16 February 2011.

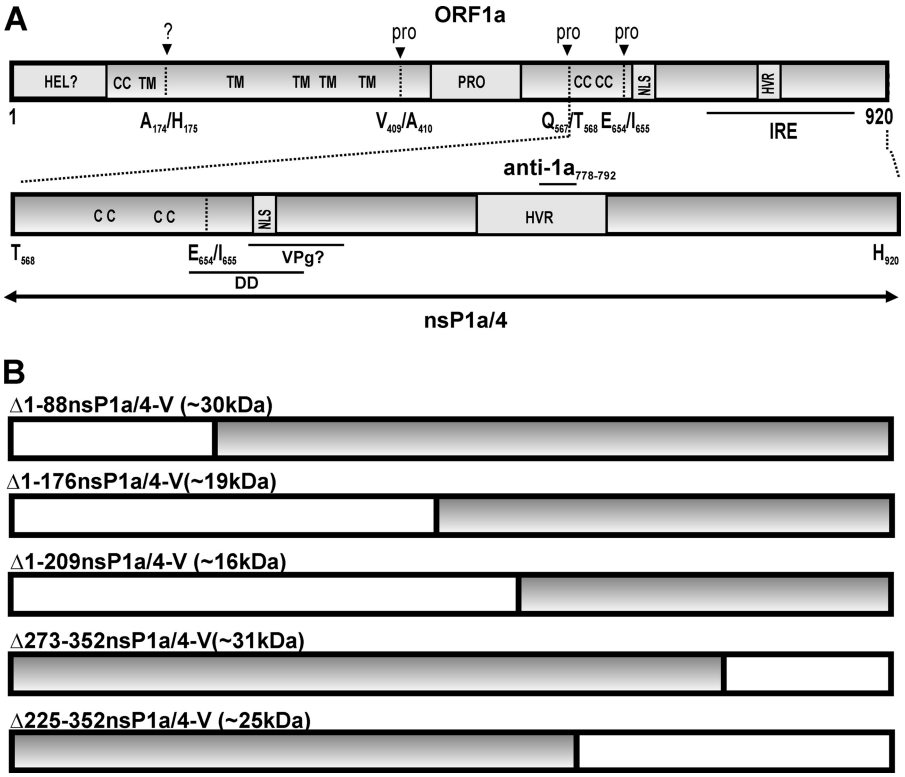

FIG. 1. (A) Schematic depiction of HAstV nsP1a polyprotein. Predicted transmembrane helices (TM), protease motif (PRO), predicted nuclear localization signal (NLS), immunoreactive epitope (IRE), predicted helicase domain (HEL), coiled-coil structures (CC), predicted death domain (DD), predicted genome-linked protein (VPg) and hypervariable region (HVR) are indicated. Arrowheads refer to putative identified proteolytic cleavage sites, which seem to be dependent on both cellular proteases (?) and the viral protease (pro). The enlarged fragment corresponds to nsP1a/4 and has been cloned into a recombinant baculovirus. (B) Schematic representation of nsP1a/4 truncated forms cloned into recombinant baculoviruses.

showed a colocalization of the nsP1a/4 with the endoplasmic reticulum and viral RNA and revealed a role of this protein in RNA replication, as well as a relationship between the genetic diversity within the HVR of the nsP1a/4 coding region and the virus replication phenotype (7, 8). Two patterns of replication that are associated with the nsP1a/4 genotype have been described: genotypes IV and V show higher levels of subgenomic RNA and lower levels of antigenomic RNA than genotypes VI and XII (8).

To better understand the role of these nsP1a/4 HVR-derived genotypes in viral replication, their interaction with the viral RNA polymerase has been analyzed in the baculovirus system. We show that nsP1a/4 is a phosphoprotein that interacts with the viral polymerase.

MATERIALS AND METHODS

Cells and viruses. *Sf*9 cells were grown at 28°C in TC100 medium (Gibco) containing 10% heat-inactivated fetal bovine serum (FBS) and 100,000 IU of penicillin and 100,000 μg of streptomycin per liter. Baculovirus stocks were prepared by infecting *Sf*9 cells at a multiplicity of infection (MOI) of 0.1 and allowing the infection to proceed for 5 to 7 days. Viruses were harvested from the culture medium after centrifugation at 1,000 × *g* to discard cell debris. Viruses were titrated by a plaque assay and stored at 4°C.

Design of recombinant baculoviruses. The Bac to Bac (Invitrogen) baculovirus expression system was used to express HAstV nsP1a/4 coding regions corresponding to genotypes IV, V, VI, and XII, several truncated forms of the nsP1a/4 genotype V coding region (Fig. 1), and the RdRp gene. The template used for the amplification of nsP1a/4 genotype XII and RdRp coding sequences was the plasmid pAVIC6 (kindly provided by S. Matsui, Gastroenterology Section, Veterans Administration Palo Alto Health Care System, Palo Alto, CA), which contains the full genome of HAstV-1. The templates used for the amplification of nsP1a/4 genotypes IV, V, and VI were the previously described plasmids pAVIC-IV, pAVIC-V, and pAVIC-VI (8), which contain the nsP1a/4 coding region of genotypes IV, V, and VI, respectively. The primers used to amplify all these sequences are shown in Table 1. PCR-amplified fragments flanked by NotI and PstI restriction enzyme sites were ligated into NotI/PstI-digested pFastBAC (Invitrogen) baculovirus transfer vector and transformed into DH10Bac competent cells, which contain bacmid DNA. Colonies containing recombinant bacmids were identified by disruption of the *lacZ*α gene. High-molecular-weight DNA minipreps were prepared from selected colonies, and the released DNA was used to transfect *Sf*9 cells with Cellfectin (Invitrogen). Recombinant baculoviruses, i.e., *Autographa californica* multiple nucleopolyhedrovirus (AcNPV)-nsP1a/4-IV, AcNPV-nsP1a/4-V, AcNPV-Δ1-88nsP1a/4-V, AcNPV-Δ1-176nsP1a/4-V, AcNPV-Δ1-209nsP1a/4-V, AcNPV-Δ273-352nsP1a/4-V, AcNPV-Δ225-352nsP1a/4-V, AcNPV-nsP1a/4-VI, AcNPV-nsP1a/4-XII, and AcNPV-Pol, were collected from the supernatants of transfected cells and stored at 4°C.

For the sake of clarity, only results generated with AcNPV-nsP1a/4-V and AcNPV-nsP1a/4-XII, used as models for the different genotypes, and those with the truncated forms are presented throughout this work. Occasionally, when remarkable differences between genotypes other than V and XII exist, the comparative results are shown.

Production of astrovirus recombinant proteins. For the heterologous protein synthesis, confluent *Sf9* cells (1.2×10^7 cells in 75-cm^2 flasks) were infected with recombinant baculovirus at an MOI of 3 and incubated at 28°C. At 72 h postinfection, cells were harvested by centrifugation (1,000 × *g* for 10 min), washed once with phosphate-buffered saline (PBS), and resuspended in two different lysis buffers (at a rate of 10^7cells/ml) depending on the downstream applications. For coimmunoprecipitation and gel filtration studies, cells were resuspended in lysis buffer containing Nonidet-P40 detergent (NP-40) (10 mM Na_2HPO_4 [pH

TABLE 1. Oligonucleotides used for designing of recombinant baculoviruses[a]

Primer sequence (5′–3′)	Construct
Forward primers	
GTCGG**GCGGCCGC**CACCATGGGTACTAATACTGGGTACACTGGAGGTGC	nsP1a/4 -IV
GTCGG**GCGGCCGC**CACCATGGGTACTAACACTGGGTACACTGGAGGTGC	nsP1a/4-V
GTCGG**GCGGCCGC**CACCATGGGTACTAATACTGGATATACCGGAGGGGC	nsP1a/4-VI
GTCGG**GCGGCCGC**CACCATGGGTACTAACACTGGGTATACTGGAGGTGC	nsP1a/4-XII
AGATG**GCGGCCGC**CACCATGGGTATCAATGGGATACTTGCACCATTTCT	Δ1-88nsP1a/4-V
GATGG**GCGGCCGC**CACCATGGGTGTAGAATTTACTGAAGTGAT	Δ1-176nsP1a/4-V
GCCCC**GCGGCCGC**CACCATGGGTCAACCACTTGATTTGTCTCA	Δ1-209nsP1a/4-V
GTCGG**GCGGCCGC**CACCATGGGTACTAACACTGGGTACACTGGAGGTGC	Δ273-352nsP1a/4-V
	Δ225-352nsP1a/4-V
GAAGG**GCGGCCGC**CACCATGGTTATCAAAAAACAAGGCCCCAAAAAACT	Polymerase
Reverse primers	
AACAA**CTGCAG**CTAACCTAATGAGTGGTAATTTTGGGCCCCT	nsP1a/4 –IV
	nsP1a/4-V
	nsP1a/4-VI
	nsP1a/4-XII
	Δ1-88nsP1a/4-V
	Δ1-176nsP1a/4-V
	Δ1-209nsP1a/4-V
TGCCTT**CTGCAG**CTAGTGTGGCGCTGGCAGAATAAACTT	Δ273-352nsP1a/4-V
CGCCAC**CTGCAG**CTATTGTTCTGGTTGTTTCTCTT	Δ225-352nsP1a/4-V
TTATTG**CTGCAG**CTAGCCATCACACTTCTTTGGTCCTCCCC	Polymerase

[a] NotI and PstI restriction sites are shown in boldface type, and the Kozak sequence used is underlined.

7.5], 150 mM NaCl, 2 mM EDTA, 1% [vol/vol] NP-40, 5 μg/μl leupeptin, and 5 μg/μl aprotinin) and incubated at 4°C for 30 min. Cell lysates were then centrifuged at 14,000 × *g* for 15 min at 4°C, and cell debris was discarded. For other applications, cells harvested by centrifugation were resuspended in lysis buffer containing sodium dodecyl sulfate (SDS) (62.5 mM Tris-HCl [pH 6,8], 2% [by volume] SDS, 5 μg/μl leupeptin, and 5 μg/μl aprotinin). Extracts obtained from *Sf9* cells infected with a polyhedrin-negative baculovirus strain (AcNPVRP8) were used as negative controls of expression.

Antibody production. Polyclonal antibody directed against the HAstV RNA-dependent RNA polymerase (anti-$Pol_{1217–1232}$) was prepared using a synthetic peptide coupled to keyhole limpet hemocyanin (KLH) as an immunogen. A synthetic peptide, spanning amino acid positions 1216 to 1232 from GenBank accession no. L23513 (NFINKDQREKYRHVHE), was designed taking into account the results of a hydrophilicity analysis using the ProtScale program available at http://ca.expasy.org/cgi-bin/protscale.pl and based on the method described by Hopp and Woods (10). Samples (25 μg) of this peptide covalently linked to KLH were administered to 8-week-old female Swiss mice in the presence of Freund's complete adjuvant and following a previously described schedule (26). Antigen was intraperitoneally injected at weeks 0, 2, 3, 4, and 5, and between weeks 4 and 5 and thereafter ascitic fluids were collected and processed. All animal manipulations were performed following a standardized and officially approved protocol (Generalitat de Catalunya 2963) and under the supervision of the Experimental Animal Ethics Committee of the University of Barcelona.

Immunoblotting analysis. Recombinant proteins were analyzed by sodium dodecyl sulfate-polyacrylamide gel electrophoresis (SDS-PAGE) and Western blotting (WB). In most experiments, samples were boiled in Laemmli buffer (1 M Tris-HCl [pH 6.8], 40% glycerol, 25% β-mercaptoethanol, 1% SDS, and 0.05% bromophenol blue), electrophoresed in an SDS–10% polyacrylamide gel, and blotted onto a nitrocellulose membrane. In some experiments, samples were not denatured before SDS-PAGE in order to compare their mobility under denaturing or semidenaturing conditions. After being blocked with 5% skim milk-TBS buffer (50 mM Tris-HCl [pH 7.6] and 100 mM NaCl), membranes were incubated with either an anti-$1a_{778–792}$ mouse polyclonal antibody (7) or an anti-$Pol_{1216–1232}$ mouse polyclonal antibody and revealed with a secondary anti-mouse immunoglobulin G (IgG) alkaline phosphatase-conjugated antibody (Calbiochem) in some experiments and a peroxidase-conjugated antibody (Amersham) in others. The enzyme reaction was developed by adding nitroblue tetrazolium–5-bromo-4-chloro-3-indolylphosphate (NBT-BCIP) (Roche) or SuperSignal West Femto (Pierce), respectively.

Coimmunoprecipitation. *Sf9* cells (1.2×10^7 cells in 75-cm^2 flasks) were coinfected with the baculovirus encoding the RdRp (AcNPV-Pol) and one of each baculovirus encoding the different nsP1a/4 proteins (AcNPV-nsP1a/4-V, AcNPV-nsP1a/4-VI, and AcNPV-nsP1a/4-XII) or one of each of the baculoviruses bearing the truncated forms of the nsP1a/4 coding region (AcNPV-Δ1-88nsP1a/4-V, AcNPV-Δ1-176nsP1a/4-V, AcNPV-Δ1-209nsP1a/4-V, AcNPV-Δ273-352nsP1a/4-V, AcNPV-Δ225-352nsP1a/4-V) at an MOI of 1 for each virus. At 72 h postinfection, cells were lysed as described above with a cell lysis buffer containing NP-40 and the extracts were incubated for 1 h at 4°C with either the anti-$Pol_{1217–1232}$ mouse polyclonal antibody diluted 1:100 or a nonimmune ascitic fluid (anti-FCA). Immune complexes were harvested by the addition of 50 μl of protein A-agarose (Roche) and 3 h of incubation at 4°C, followed by centrifugation at 12,000 × *g* for 20 s. Pellets were subjected to three washes of 20 min at 4°C, first with lysis buffer, second with a high-salt buffer (10 mM Na_2HPO_4 [pH 7.5], 500 mM NaCl, 0,1% [vol/vol] NP-40, 5 μg/μl leupeptin, and 5 μg/μl aprotinin), and third with a low-salt buffer (10 mM Na_2HPO_4 [pH 7.5], 0,1% [vol/vol] NP-40, 5 μg/μl leupeptin, and 5 μg/μl aprotinin). Finally, the immune complexes were resuspended in 50 μl of 1× Laemmli buffer, boiled for 5 min, and centrifuged at 12,000 × *g* for 20 s. Supernatants were subjected to SDS–10% PAGE and examined by Western blot analysis with a 1:250 dilution of the anti-$1a_{778–792}$ mouse polyclonal antibody. As negative controls, immunoprecipitation of extracts from cells singly infected with AcNPV-nsP1a/4-V, AcNPV-nsP1a/4-VI, or AcNPV-nsP1a/4-XII with the anti-$Pol_{1216–1232}$ mouse polyclonal antibody diluted 1:100 was also performed.

Detection of phosphorylated and glycosylated proteins. *Sf9* cells (1.2×10^7 cells in 75-cm^2 flasks) were infected with recombinant baculovirus expressing the nsP1a/4-V protein (AcNPV-nsP1a/4-V) at an MOI of 3 and incubated at 28°C. At 72 h postinfection, the presence of phosphorylated proteins, among those immunoprecipitated with the anti-$1a_{778–792}$ polyclonal antiserum, was analyzed by Western blotting, using a monoclonal anti-phosphoserine/threonine antibody (anti-$^PS^PT$) (BD Biosciences Pharmingen). The immunoprecipitation assay was performed under the same conditions described above. The glycosylation state was also tested on transferred membrane proteins by oxidizing the carbohydrate moieties with 10 mM sodium periodate, followed by incorporation of biotin hydrazide. Biotinylated complexes were detected by a streptavidin-alkaline phosphatase (Sigma). Ovoalbumin was used as a positive control of a glycosylated protein.

Staurosporine treatment. Confluent *Sf9* cells (3×10^6 cells in 10-cm^2 wells) were infected with recombinant baculovirus expressing the nsP1a/4-V protein (AcNPV-nsP1a/4-V) at an MOI of 3 and incubated at 28°C. At 18 h postinfection, cells were treated with staurosporine at 35, 50, and 100 nM concentrations for 6 h. Thereafter, cells were washed once in PBS, lysed with an SDS-containing buffer, and analyzed by immunoblotting using the anti-$1a_{778–792}$ antibody. The level of staurosporine phosphorylation inhibition was measured by quantifying the ratio of band intensities using Quantity One software (Bio-Rad).

nsP1a/4 protein expression under phosphate starvation. Confluent *Sf9* cells (3×10^6 cells in 10-cm^2 wells) were infected with recombinant baculovirus

expressing the nsP1a/4-V protein (AcNPV-nsP1a/4-V) at an MOI of 3 and incubated at 28°C. At 18 h postinfection, a phosphate-deficient TC100 medium was added, and at 48 h postinfection, cells were washed once in PBS, lysed with an SDS-containing buffer, and analyzed by immunoblotting using the anti-$1a_{778–792}$ antibody. The level of phosphorylation inhibition was measured by quantifying the ratio of band intensities using Quantity One software.

Protein labeling with [^{32}P]orthophosphate. Confluent *Sf9* cells (3×10^6 cells in 10-cm^2 wells) were infected with recombinant baculovirus expressing the nsP1a/4-V protein (AcNPV-nsP1a/4-V) at an MOI of 3 and incubated at 28°C. At 18 h postinfection, cells were starved for 1 h using phosphate-deficient TC100 medium. Cells were then labeled for 24 h with 125 μCi phosphorus-32 (Amersham) in 1 ml starvation medium. Finally, cells were washed once in PBS, lysed with an SDS-containing buffer, and analyzed by SDS–10% PAGE and revealed by exposing a phosphorimaging screen.

Size exclusion chromatography. Gel filtration through Sephadex G-100 was performed with an in-house column (0.65 by 15.50 cm) equilibrated with a phosphate buffer (10 mM Na_2HPO_4 [pH 7.5], 150 mM NaCl). Three hundred μl of cell extracts (1.2×10^7 infected cells) were loaded onto the column, and 300-μl fractions were collected at a flow rate of 0.3 ml/min under room pressure conditions. Aliquots of each fraction were subjected to SDS–10% PAGE, and Western blot analyses with anti-$1a_{778–792}$ or anti-$Pol_{1217–1232}$ mouse polyclonal antibodies were performed for the detection of the nsP1a/4 proteins or the polymerase, respectively. The column was calibrated with known molecular weight standards: immunoglobulin G (IgG) (150 kDa), bovine serum albumin (BSA) (66 kDa), ovoalbumin (OA) (43 kDa), and lysozyme (LZ) (14 kDa).

RESULTS

Production of astrovirus nsP1a/4 and RdRp in insect cells. The potential interaction of nsP1a/4 protein and the viral polymerase was analyzed through baculovirus-expressed proteins. Different nsP1a/4 protein variants, including different genotypes and several amino- and carboxy-truncated forms (Fig. 1), as well as the viral polymerase were produced. Immunoreactive bands of expected sizes were detected, with approximate molecular masses of 40 to 42 kDa (depending on the genotype) for the nsP1a/4 (Fig. 2A; only results for genotypes V and XII are shown) and 61 kDa for the polymerase (Fig. 2B). Truncated nsP1a/4 proteins of the expected size, with approximate molecular masses of 30 kDa, 19 kDa, 16 kDa, 31 kDa, and 25 kDa for the Δ1-88nsP1a/4-V, Δ1-176nsP1a/4-V, Δ1-209nsP1a/4-V, Δ273-352nsP1a/4-V, and Δ225-352nsP1a/4-V, respectively, were also detected (Fig. 2C). No immunoreactive bands were detected in polyhedrin-negative AcNPVRP8-infected *Sf9* cells.

Recombinant nsP1a/4 is phosphorylated. Expression of nsP1a/4 proteins also produced protein bands of higher molecular masses than expected: 50 kDa for nsP1a/4-IV (data not shown), nsP1a/4-V, and nsP1a/4-XII proteins (Fig. 2A), 53 kDa for nsP1a/4-VI (data not shown), and in the range 19 to 37 kDa for the truncated proteins (Fig. 2C). Since computational analysis of the nsP1a/4 protein predicts several putative phosphorylation and O-glycosylation sites, the observed increases in the molecular weight could be due to posttranslational modifications such as the addition of phosphate or carbohydrate moieties. To elucidate whether phosphorylation occurs, recombinant nsP1a/4-V proteins, used as models, were immunoprecipitated with the anti-$1a_{778–792}$ antibody and detected using the anti-$^{P}S^{P}T$ antibody. One phosphoprotein of around 50 kDa was detected (Fig. 3A), indicating that phosphorylation is indeed a posttranslational modification of the nsP1a/4-V protein. To verify the second possibility, the potential carbohydrates present in the nsP1a/4 proteins were oxidized and the newly arising radicals were biotinylated and detected with streptavidin. Since no positive bands were observed (data not shown) it was concluded that glycosylation is not a major posttranslational modification.

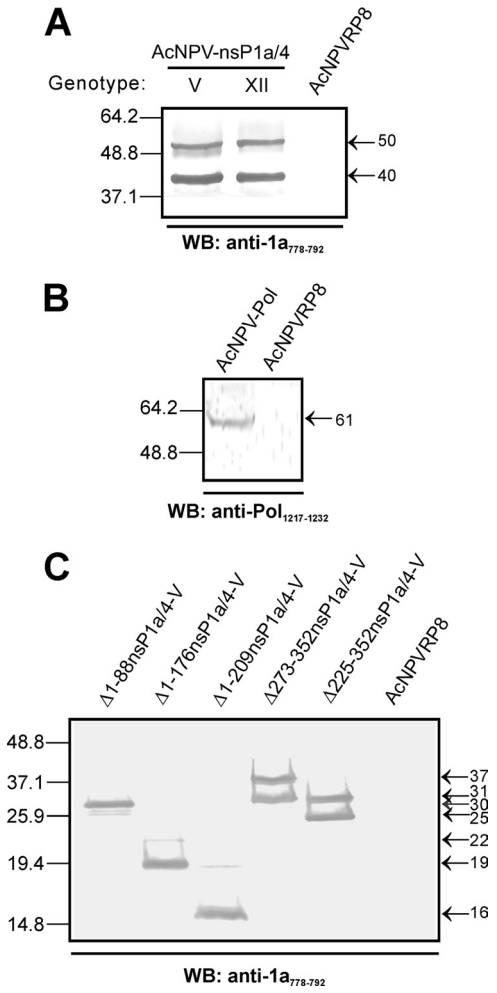

FIG. 2. Western blot analysis with antibodies against the nsP1a/4 protein (anti-$1a_{778–792}$ antibody) and the polymerase (anti-$Pol_{1217–1232}$ of cell extracts of *Sf9* cells infected with recombinant baculoviruses expressing nsP1a/4 proteins corresponding to genotypes V and XII (AcNPV-nsP1a/4-V, AcNPV-nsP1a/4-XII) (A), the polymerase (AcNPV-Pol) (B), or different truncated forms of nsP1a/4-V protein (AcNPV-Δ1-88nsP1a/4-V, AcNPV-Δ1-176nsP1a/4-V, AcNPV-Δ1-209nsP1a/4-V, AcNPV-Δ273-352nsP1a/4-V, and AcNPV-Δ225-352nsP1a/4-V) (C). As negative controls, extracts from polyhedrin-negative baculovirus (AcNPVRP8)-infected cells were included. Positions of molecular size markers (in kilodaltons) are indicated on the left, and molecular weights of recombinant proteins are on the right.

In order to confirm the phosphorylated state of the proteins, *Sf9* cells infected with AcNPV-nsP1a/4-V, as a model genotype, were treated with staurosporine, a potent inhibitor of protein kinase C, and a wide variety of other enzymes of both serine/threonine and tyrosine kinase families (19, 28). Cell extracts obtained at 24 h postinfection (18 h in the absence of the drug and 6 h in the presence of the drug) were analyzed by Western blotting with the anti-$1a_{778–792}$ antibody. As shown in Fig. 3B, treatment with staurosporine resulted in a decrease in the levels of the 50-kDa form of the nsP1a/4-V protein in a dose-dependent manner, suggesting that the protein was phos-

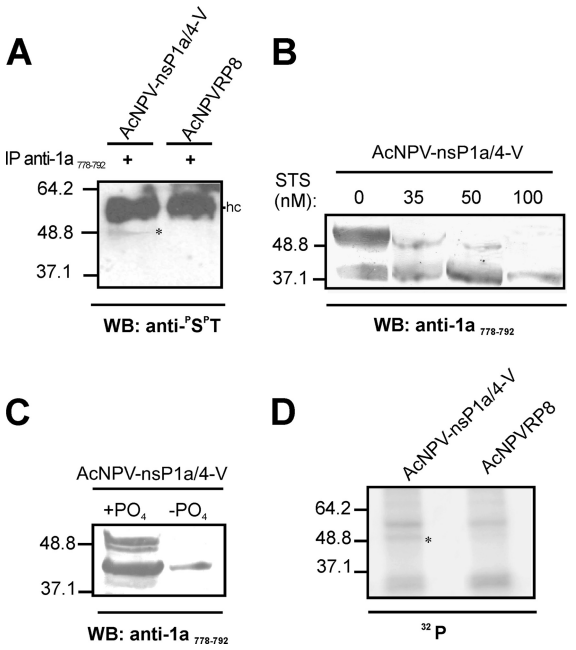

FIG. 3. Analysis of the phosphorylation state of the nsP1a/4-V protein expressed in insect cells. (A) Western blot analysis, with an antibody against phosphoserines and phosphothreonines (anti-$^{P}S^{P}T$), of a cell extract from *Sf9* cells infected with the AcNPV-nsP1a/4-V recombinant baculovirus, previously immunoprecipitated with the anti-$1a_{778–792}$ antibody (lane 1). As a negative control the same procedure was applied to an extract of cells infected with the polyhedrin-negative baculovirus strain AcNPVRP8 (lane 2) (B) Effect of staurosporine (STS) on the synthesis and phosphorylation of nsP1a/4-V protein expressed in insect cells. *Sf9* cells were infected with recombinant baculovirus AcNPV-nsP1a/4-V and treated with staurosporine at different concentrations. After treatment, cell extracts were analyzed by Western blotting using the anti-$1a_{778–792}$ antibody. (C) Expression of nsP1a/4-V protein in *Sf9* cells using media with or without PO_4. *Sf9* cells were infected with recombinant baculovirus AcNPV-nsP1a/4-V and maintained during 48 h in media with (lane 1) or without (lane 2) PO_4. Thereafter, cell extracts were analyzed by Western blotting using the anti-$1a_{778–792}$ antibody. (D) nsP1a/4 labeling with [^{32}P]orthophosphate. *Sf9* cells infected with either a baculovirus encoding the nsP1a/4-V protein (lane 1) or the polyhedrin-negative baculovirus strain AcNPVRP8 (lane 2) were labeled with [^{32}P]orthophosphate. Proteins were resolved by SDS-PAGE, and radioactively labeled proteins were visualized by exposing a phosphorimaging screen. The position of labeled nsP1a/4-V protein is indicated by an asterisk. hc, heavy chains of the antibody used in the immunoprecipitation. Positions of molecular size markers (in kilodaltons) are indicated on the left.

phorylated (image analysis confirmed that the intensity of the nonphosphorylated 40-kDa band did not significantly decrease with drug concentrations below 100 nM, while the 50-kDa phosphorylated band already started to decrease at a drug concentration of 35 nM, reaching its maximum at 100 nM). To further confirm this observation, infection of *Sf9* cells with the AcNPV-nsP1a/4-V construct was allowed to proceed under conditions of phosphate depletion. Under such conditions, the 50-kDa form of the nsP1a/4-V protein completely disappeared (Fig. 3C). Image analyses suggested that a certain amount of the 50-kDa form ought to be present (considering the amount of the 40-kDa nonphosphorylated form and the usual ratio of nonphosphorylated/phosporylated isoforms) provided that phosphorylation inhibition does not occur. The concluding

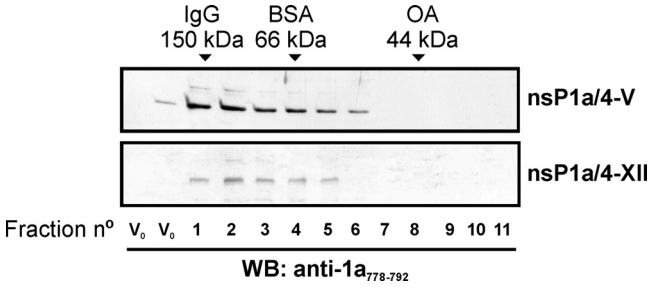

FIG. 4. Sephadex G-100 gel filtration of nsP1a/4 proteins corresponding to genotypes V and XII. Western blot analysis with the anti-$1a_{778–792}$ antibody was employed for detection. The positions of the standard marker proteins immunoglobulin G (IgG), bovine serum albumin (BSA), and ovalbumin (OA) are indicated at the top. Fractions corresponding to void volume are indicated by V_0.

demonstration of nsP1a/4-V phosphorylation was through its specific labeling with [^{32}P]orthophosphate. After 24 h of replication in the presence of labeled phosphate, a single radioactive band of approximately 50 kDa was detected in extracts from AcNPV-nsP1a/4-V-infected cells but not in extracts from polyhedrin-negative AcNPVRP8-infected cells (Fig. 3D). Although the radioactive band was very faint, it must be borne in mind that the total phosphate concentration was 10,000 times lower than the usual one.

Additionally, from results observed with the truncated forms it can be concluded that the N-terminal half portion of the protein is essential for the phosphorylation process, since the phosphorylation pattern of the amino-truncated forms was completely altered compared to those of the nontruncated or the carboxy-truncated proteins (Fig. 2C). In the case of Δ1-88nsP1a/4-V protein, some phosphorylated forms were detected but with a number of added phosphates significantly lower than those in the nontruncated protein and the carboxy-truncated proteins, giving rise to a smaller increase in the molecular weight (see also Fig. 9). In the case of Δ1-176nsP1a/4-V and Δ1-209nsP1a/4-V proteins, phosphorylation was almost absent, although a protein of a molecular weight corresponding to a highly phosphorylated form could be detected as a faint band, indicating that either the conformation of these truncated proteins favors the accessibility of only some phosphorylation sites or that the conformation of the Δ1-88nsP1a/4-V prevents the accessibility of these sites.

Recombinant nsP1a/4 protein forms oligomers. To find out whether oligomeric forms of nsP1a/4 might exist, *Sf9* cells were infected with baculovirus expressing nsP1a/4 proteins and cell extracts were analyzed by gel filtration on a Sephadex G-100 column. The column was calibrated with four globular proteins of known molecular masses from 150 kDa to 14 kDa (IgG, BSA, OA, LZ). Regression analysis demonstrated a linear relationship between the elution volumes of the protein standards and the logarithms of their reported molecular masses (data not shown). The presence of nsP1a/4 proteins in each fraction was monitored by Western blot analysis with the anti-$1a_{778–792}$ antibody. The bulk of nsP1a/4 proteins eluted around the IgG (150 kDa) marker, with an important tail around the BSA (66 kDa) marker due to protein spreading, suggesting the predominant presence of trimers or larger oligomers and, to a lesser extent, dimers (Fig. 4; only results from genotypes V and

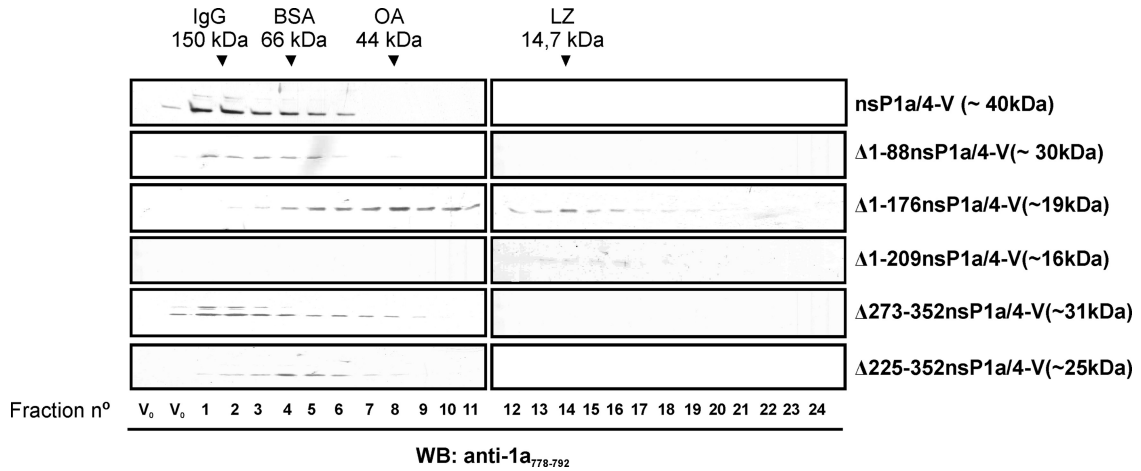

FIG. 5. Sephadex G-100 gel filtration of nsP1a/4-V protein and its truncated forms. Western blot analysis with the anti-$1a_{778–792}$ antibody was employed for detection. The positions of the standard marker proteins immunoglobulin G (IgG), bovine serum albumin (BSA), ovalbumin (OA), and lysozime (LZ) are indicated at the top. Fractions corresponding to void volume are indicated by V_0.

XII are shown). The nonphosphorylated isoform of the protein was the predominant one in the oligomers (Fig. 4).

The central part of the nsP1a/4 protein contains an oligomerization domain. The distinct N-terminal and C-terminal truncated forms of the nsP1a/4-V protein were examined to determine the region of nsP1a/4 protein involved in oligomerization. Lysates from *Sf9* cells infected with each of these baculoviruses were loaded onto the columns, and fractions were collected. Immunoblot analyses of fractions indicated that Δ1-88nsP1a/4-V, Δ1-176nsP1a/4-V, Δ1-209nsP1a/4-V, Δ273-352nsP1a/4-V, and Δ225-352nsP1a/4-V proteins eluted at fractions equivalent to molecular masses of around 50 to 150, 10 to 60, 10 to 20, 50 to 150, and 50 to 75 kDa, respectively (Fig. 5). Since their predicted monomeric molecular masses are 30, 19, 16, 25, and 31 kDa, respectively, their elution profiles demonstrated that the predominant forms were monomers for Δ1-209nsP1a/4-V, monomers, dimers and trimers for Δ1-176nsP1a/4-V and dimers, trimers and higher oligomers for Δ1-88nsP1a/4-V, Δ273-352nsP1a/4-V, and Δ225-352nsP1a/4-V. The oligomeric state of the different forms of the nsP1a/4-V protein was also analyzed through the mobility of nondenatured extracts in SDS-PAGE (Fig. 6). Under these semidenaturing conditions, the nsP1a/4-V protein resolved mainly as monomers and trimers and likely higher forms which would not be detected in these gels, whose upper limit is of around 120 kDa (Fig. 6A): the Δ1-88nsP1a/4-V protein as monomers, dimers, trimers, and higher forms (Fig. 6B); the Δ1-176nsP1a/4-V protein as monomers, tetramers, and higher forms (Fig. 6B); the Δ1-209nsP1a/4-V protein as monomers (Fig. 6B); the Δ273-352nsP1a/4-V protein as monomers and likely higher forms (Fig. 6B) not detectable in these gels; and the Δ225-352nsP1a/4-V protein as monomers, dimers, and higher forms (Fig. 6B). These results suggest that the region between amino acids 176 and 209 contains an oligomerization domain. However, since oligomerization is less optimal for the Δ1-176nsP1a/4-V mutant than for the Δ1-88nsP1a/4-V, the domain is likely to be larger. Alternatively, the occurrence of a second oligomerization domain between residues 88 and 176 could also explain this behavior.

nsP1a/4 protein interacts with the viral polymerase. The involvement of nsP1a/4 in viral RNA replication as well as its interaction with the endoplasmic reticulum (7, 8) suggests that this protein may be an integral part of the viral replication complex interacting with the RNA polymerase. The potential interaction between nsP1a/4 and RNA polymerase was studied through coimmunoprecipitation of these proteins from ex-

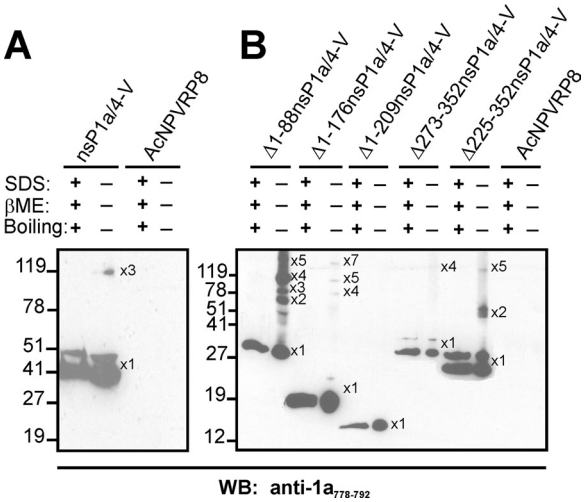

FIG. 6. Western blot analysis with the anti-$1a_{778–792}$ antibody of denatured versus nondenatured extracts of nsP1a/4-V protein and their truncated forms. Extracts from *Sf9* cells infected with the AcNPV-nsP1a/4-V (A) or the AcNPV-Δ1-88nsP1a/4-V, AcNPV-Δ1-176nsP1a/4-V, AcNPV-Δ1-209nsP1a/4-V, AcNPV-Δ273-352nsP1a/4-V, and AcNPV-Δ225-352nsP1a/4-V (B) baculoviruses were denatured using standard procedures (SDS, β-mercaptoethanol [βME], and boiling) or nondenatured. In both cases samples were run under denaturing conditions (SDS-PAGE) and thus the whole procedure was considered denaturing or semidenaturing, respectively. As negative controls, extracts from polyhedrin-negative baculovirus (AcNPVRP8)-infected cells were included. Positions of molecular size markers (in kilodaltons) are indicated on the left. The different oligomeric states are indicated by ×1 (monomers), ×2 (dimers), ×3 (trimers), and successively.

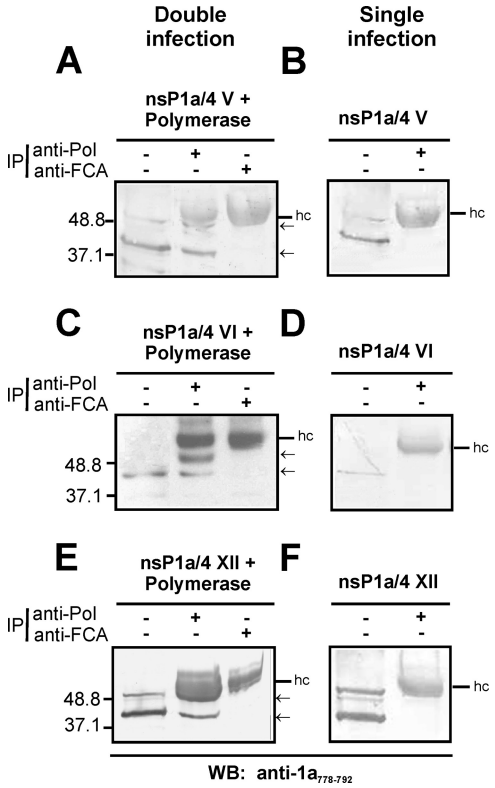

FIG. 7. Coimmunoprecipitation of the RNA polymerase and nsP1a/4 proteins corresponding to genotypes V (A and B), VI (C and D), and XII (E and F). Cell extracts from double-infection (AcNPV-Pol with either AcNPV-nsP1a/4-V, AcNPV-nsP1a/4-VI, or AcNPV-nsP1a/4-XII) experiments were immunoprecipitated with either the anti-$Pol_{1217–1232}$ antibody or a nonimmune ascitic fluid (anti-FCA) (A, C and E). Cell extracts from single-infection (AcNPV-nsP1a/4-V, AcNPV-nsP1a/4-VI, or AcNPV-nsP1a/4-XII) experiments were immunoprecipitated with the anti-$Pol_{1217–1232}$ antibody (B, D, and F) as controls for the specificity of the immunoprecipitation reaction. Immunoprecipitates were resolved by SDS-PAGE, transferred to nitrocellulose membranes, and probed with the anti-$1a_{778–792}$ antibody. Nonimmunoprecipitated cell extracts are shown in lane 1 of each panel. Coimmunoprecipitated proteins as well as the heavy chains of the antibody used in the immunoprecipitation are marked by arrows and hc, respectively. Molecular size marker positions are indicated on the left.

tracts of *Sf9* cells coinfected with two baculoviruses encoding the HAstV nsP1a/4 and the RNA polymerase. At 72 h postinfection, cells were lysed with a mild detergent and immunoprecipitated with anti-$Pol_{1217–1232}$. An immunoprecipitation with a nonrelated antibody (anti-Freund's complete adjuvant [anti-FCA]) was used as a negative control. Subsequent Western blot analyses with anti-$1a_{778–792}$ antibody revealed that nsP1a/4 proteins could be specifically pulled down from the cell lysate (Fig. 7). It is noteworthy that both phosphorylated and nonphosphorylated forms of nsP1a/4 protein interacted with the viral RNA polymerase for all genotype-derived proteins (only genotypes V, VI, and XII are shown), and even in the case of nsP1a/4-VI the phosphorylated isoforms showed a higher binding capacity (Fig. 7C). The specificity of the interaction was confirmed after immunoprecipitation with anti-$Pol_{1217–1232}$ of extracts from cells infected only with the AcNPV-nsP1a/4-V, the AcNPV-nsP1a/4-VI, or the AcNPV-nsP1a/4-XII recombinant viruses (Fig. 7B, D, and F, respectively), since no proteins were pulled down.

The nsP1a/4-V and RNA polymerase interaction was further studied by gel filtration analysis. For this purpose, lysates from AcNPV-nsP1a/4-V and AcNPV-Pol coinfected *Sf9* cells were loaded onto a Sephadex G-100 column and fractions were collected as described above. The presence of nsP1a/4 protein and RNA polymerase in each fraction was evaluated by Western blotting using the anti-$1a_{778–792}$ and anti-$Pol_{1217–1232}$ antibodies, respectively. The elution pattern obtained from cells coinfected with AcNPV-nsP1a/4-V and AcNPV-Pol baculoviruses was different from that obtained from cells infected with the AcNPV-nsP1a/4-V or AcNPV-Pol alone. The nsP1a/4-V protein expressed alone eluted in a wider range of fractions (50 to 150 kDa) than when expressed in combination with the RNA polymerase (75 to 150 kDa) (Fig. 8A). This change could be explained by a lower concentration of nsP1a/4-V protein in double-infected cells than in mono-infected cells and, in consequence, in a much lower tail spread of the protein during the chromatography. However, the most striking change was that of the polymerase which was recovered in those fractions corresponding to a molecular mass of around 65 to 70 kDa (the predicted molecular mass is 61 kDa) when expressed alone (Fig. 8B), and in those fractions corresponding to a molecular mass of around 100 to 110 kDa when expressed in combination with nsP1a/4-V protein (Fig. 8B). This change in the polymer-

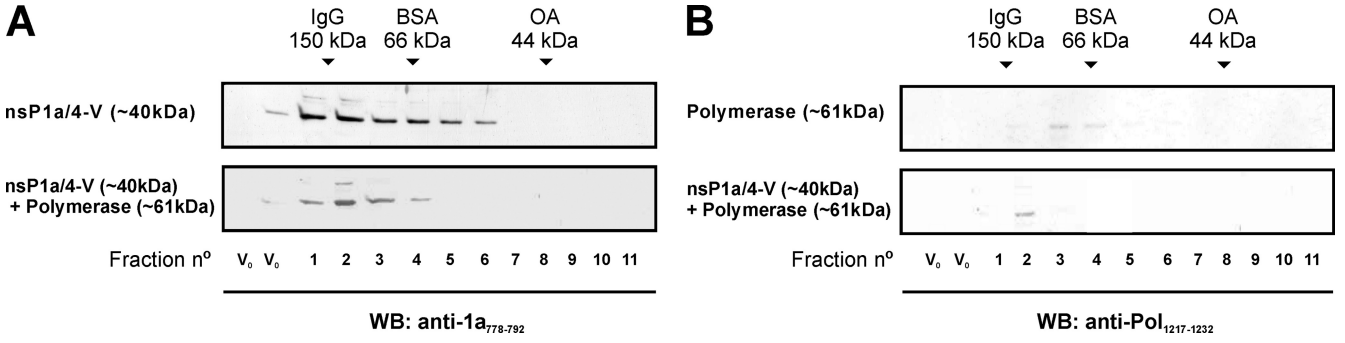

FIG. 8. Sephadex G-100 gel filtration of cell extracts from insect cells single infected or double infected with AcNPV-nsP1a/4-V and AcNPV-Pol. Collected fractions were subjected to Western blotting with the anti-$1a_{778–792}$ antibody (A) and the anti-$Pol_{1217–1232}$ antibody (B). Positions of standard marker proteins immunoglobulin G (IgG), bovine serum albumin (BSA), and ovalbumin (OA) are indicated at the top. Fractions corresponding to void volume are indicated by V_0.

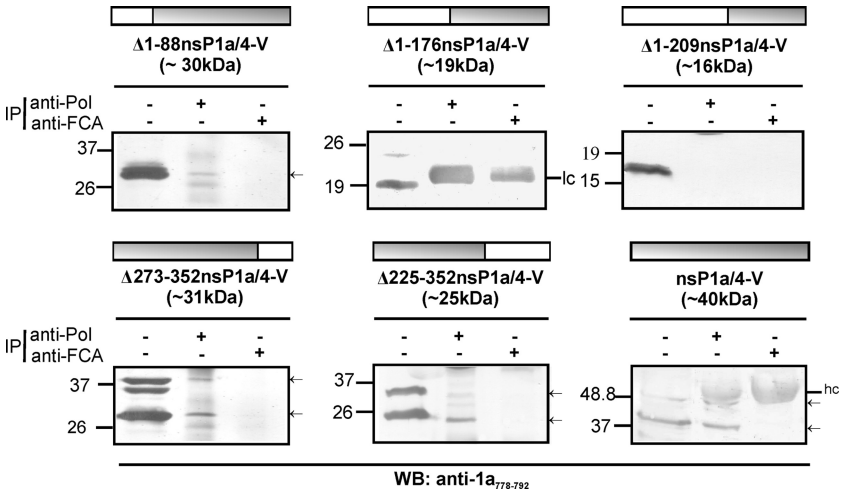

FIG. 9. Coimmunoprecipitation of the RNA polymerase and truncated forms of the nsP1a/4 protein. Cell extracts obtained from coinfection experiments with recombinant baculovirus expressing the AcNPV-Pol and the different truncated forms of nsP1a/4 (AcNPV-Δ1-88nsP1a/4-V, AcNPV-Δ1-176nsP1a/4-V, AcNPV-Δ1-209nsP1a/4-V, AcNPV-Δ273-352nsP1a/4-V, and AcNPV-Δ225-352nsP1a/4-V) were incubated with either the anti-$Pol_{1217–1232}$ antibody or a nonimmune ascitic fluid (anti-FCA). Immunoprecipitates were resolved by SDS-PAGE, transferred to nitrocellulose membranes, and probed with anti-$1a_{778–792}$ antibody. Nonprecipitated cell extracts are shown in lane 1 of each panel. Coimmunoprecipitated proteins and the light chains of the antibody used to immunoprecipitate are marked by arrows and lc, respectively. hc, heavy chain. Molecular size marker positions are indicated on the left.

ase elution pattern could be explained by the occurrence of a heterodimer formed through the interaction of both proteins, consistent with results of the coimmunoprecipitation assays (Fig. 7). An additional and remarkable observation was that the phosphorylated form of nsP1a/4-V protein could also be detected in those fractions corresponding to a heterodimer, indicating that this form can also interact with the RNA polymerase (Fig. 8A) as shown above with the coimmunoprecipitation experiments (Fig. 7).

To clarify which domain of the nsP1a/4 protein is involved in the interaction with the RNA polymerase, the full-length RNA polymerase was coexpressed in insect cells with the distinct nsP1a/4-V deletion mutants. Immunoprecipitation experiments were performed using the anti-$Pol_{1217–1232}$ antibody to pull down proteins and the anti-$1a_{778–792}$ antibody in the immunoblotting analysis. Interestingly, the Δ1-176nsP1a/4-V and Δ1-209nsP1a/4-V truncated forms completely failed to interact with the RNA polymerase (Fig. 9). These results suggest that the region spanning amino acids 88 to 176 contains essential sequences for interaction with the RNA polymerase.

DISCUSSION

Small viruses have evolved to maximize their genomic information by producing multifunctional viral proteins. To expand the information stored in the small viral genome, the cleavage end products and their precursors may have distinct functions. The putative nsP1a/4 or C-terminal nsP1a protein of astrovirus is an example of this. The exact functions of the nonstructural proteins encoded in ORF1a of astrovirus, with the exception of the protease, still remain elusive. Among them, the nsP1a/4 has received special attention and has been suggested to be involved in many different roles, including apoptosis induction (6), in order to activate those caspases necessary for capsid maturation (3, 6, 20), and regulation of RNA replication (8). Related with these functions it is remarkable that nsP1a/4 protein contains two essential domains, a DD (6) and a VPg (1), which may be associated with the induction of apoptosis and genome replication, respectively. Additionally, an HVR, whose variability affects genome replication (8, 9), is also present in this protein (22, 25, 29). Although the exact boundaries of the proteolytical cleavages of the ORF1a are not well identified, our initial working hypothesis was that a first cleavage at position Gln-567/Thr-568 (14) would render the nsP1a/4 protein of around 40 kDa and that further unknown processes of this protein would render smaller proteins. Some of these proteins are in the range of 21 to 27 kDa and include phosphorylated forms (7). The crystal structure of the astrovirus protease has very recently been described (27), suggesting a high preference for Glu and Asp at the P1 substrate position and consequently a preference for the Glu-654/Ile-655 cleavage rather than the Gln-567/Thr-568 cleavage and even suggesting that these latter residues are located in the S1 pocket. However, the inclusion of the coiled-coil domain predicted in the region Thr-568–Glu-654 is of high interest and justifies the construct corresponding to what we call nsP1a/4 protein. Additionally, the truncated form Δ1-88nsP1a/4-V corresponds exactly to the protein originated after the Glu-654/Ile-655 cleavage.

To better understand the role of the nsP1a/4 HVR-derived genotypes in viral replication, their potential interaction with the viral RNA polymerase was analyzed by expressing these proteins in the baculovirus system. Expression of HVR-derived forms of the nsP1a/4 protein in insect cells resulted in high-level production of two main products, one of the expected size (40 to 42 kDa depending on the genotype) and a second one larger than expected that could contain several proteins with small molecular size differences (50- to 55-kDa range). These differences may be attributed to phosphorylation processes, since both PO_4 starvation and kinase inhibition induced a

complete loss and a concentration-dependent reduction of the proteins of higher molecular weight of the nsP1a/4-V type used as a model. In fact, these proteins are specifically labeled when produced in the presence of [^{32}P]orthophosphate and are specifically recognized by an antibody against phosphoserines and phosphothreonines. While these results are expected according to previous studies (7), smaller proteins were not observed, indicating either that no proteases able to produce the cleavages are present in baculovirus-infected insect cells or that the conformation of the nsP1a/4 protein is not adequate to allow the processing to occur. Another important point was to determine the oligomeric state of the protein and whether it could be affected by the phosphorylation state and/or the HVR type. Gel filtration and semidenaturing SDS-PAGE analysis revealed that nsP1a/4 proteins form oligomers, with trimers or higher oligomers being the predominant form. The nonphosphorylated isoform was the predominant one in the oligomers detected by gel filtration. Since the phosphorylated isoforms were not present in those fractions corresponding to monomers, it may be suggested that they are mainly in a nonglobular state. Thus, it may be postulated that the phosphorylation state regulates the conformation of these proteins from a nonglobular to an oligomeric condition or that depending on the conformation and state of oligomerization different phosphorylation patterns may occur. An oligomerization domain could be mapped between residues 176 and 209 of nsP1a/4-V, but the exact boundaries of the domain could not be determined. This domain, as well as the region spanning residues 1 to 176, contains several potential phosphorylation sites (8). An additional and intriguing point is that while the nonphosphorylated form of most of the nsP1a/4-V-derived proteins was the predominant one present in oligomers, in the Δ273-352nsP1a/4-V carboxy-truncated protein the phosphorylated forms were also present in oligomers, which were of the higher type, indicating the critical relationship between the conformation and the phosphorylated state. These findings altogether point to a cross talk regulation between the oligomerization and phosphorylation states of nsP1a/4 protein which may regulate the interaction with the RNA polymerase. In fact, nsP1a/4 protein monomers, but not higher forms, interact with the RNA polymerase, likely forming a heterodimer, and the phosphorylated isoforms appear to be strongly interactive. The polymerase interaction domain is contiguously located to the oligomerization domain in the nsP1a/4 boundaries, and even they may be partially coincident, since the use of truncated proteins represents an approximation to domain mapping, and thus a steric competition among both processes could be expected. However, phosphorylation/dephosphorylation of different residues may induce conformational changes (12) favoring one or the other process. The HVR could also play a critical role in defining these conformations, taking into consideration the differential number of serine residues which are potentially susceptible to phosphorylation as well as the differential indel pattern (8). In fact, viruses bearing nsP1a/4 proteins of genotypes VI and XII have a higher number of potential phosphoserines that have been suggested to be associated with production of higher levels of genomic RNA (8). Our results suggest that at least for genotype VI, this replication pattern might be related to the higher interactive capacity of the phosphorylated isoforms of nsP1a/4-VI with the RNA polymerase. This observation was not so evident for genotype XII since the phosphorylated form was harder to visualize due to its coincidence with the IgG heavy chains. Further studies are needed to characterize the regulation of minus and plus RNA strands as well as subgenomic RNA. However, our data prove that nsP1a/4 protein is involved in the replication complex through an interaction with the RNA polymerase, and this could be related to a potential VPg function.

ACKNOWLEDGMENTS

C. Fuentes was the recipient of a FI fellowship from the Generalitat de Catalunya. This work was supported in part by grants 2005SGR00966 and 2009SGR00024 and the Biotechnology Reference Network of the Generalitat de Catalunya.

REFERENCES

1. **Al Mutairy, B., J. E. Walter, A. Pothen, and D. K. Mitchell.** 2005. Genome prediction of putative genome-linked viral protein (VPg) of astroviruses. Virus Genes **31:**21–30.
2. **Appleton, H., and P. G. Higgins.** 1975. Letter: viruses and gastroenteritis in infants. Lancet **i:**1297.
3. **Banos-Lara, M. R., and E. Méndez.** 2010. Role of individual caspases induced by astrovirus on the processing of its structural protein and its release from the cell through a non-lytic mechanism. Virology **401:**322–332.
4. **Geigenmuller, U., T. Chew, N. Ginzton, and S. M. Matsui.** 2002. Processing of nonstructural protein 1a of human astrovirus. J. Virol. **76:**2003–2008.
5. **Gibson, C. A., J. Chen, S. A. Monroe, and M. R. Denison.** 1998. Expression and processing of nonstructural proteins of the human astroviruses. Adv. Exp. Med. Biol. **440:**387–391.
6. **Guix, S., A. Bosch, E. Ribes, L. D. Martínez, and R. M. Pintó.** 2004. Apoptosis in astrovirus-infected CaCo-2 cells. Virology **319:**249–261.
7. **Guix, S., S. Caballero, A. Bosch, and R. M. Pintó.** 2004. C-terminal nsP1a protein of human astrovirus colocalizes with the endoplasmic reticulum and viral RNA. J. Virol. **78:**13627–13636.
8. **Guix, S., S. Caballero, A. Bosch, and R. M. Pintó.** 2005. Human astrovirus C-terminal nsP1a protein is involved in RNA replication. Virology **333:**124–131.
9. **Guix, S., S. Caballero, C. Fuentes, A. Bosch, and R. M. Pintó.** 2008. Genetic analysis of the hypervariable region of the human astrovirus nsP1a coding region: design of a new RFLP typing method. J. Med. Virol. **80:**306–315.
10. **Hopp, T. P., and K. R. Woods.** 1981. Prediction of protein antigenic determinants from amino acid sequences. Proc. Natl. Acad. Sci. U. S. A. **78:**3824–3828.
11. **Jiang, B., S. S. Monroe, E. V. Koonin, S. E. Stine, and R. I. Glass.** 1993. RNA sequence of astrovirus: distinctive genomic organization and a putative retrovirus-like ribosomal frameshifting signal that directs the viral replicase synthesis. Proc. Natl. Acad. Sci. U. S. A. **90:**10539–10543.
12. **Johnson, L. N., and M. O'Reilly.** 1996. Control by phosphorylation. Curr. Opin. Struct. Biol. **6:**762–769.
13. **Jonassen, C. M., T. T. Jonassen, T. M. Sveen, and B. Grinde.** 2003. Complete genomic sequences of astroviruses from sheep and turkey: comparison with related viruses. Virus Res. **91:**195–201.
14. **Kiang, D., and S. M. Matsui.** 2002. Proteolytic processing of a human astrovirus nonstructural protein. J. Gen. Virol. **83:**25–34.
15. **Lewis, T. L., H. B. Greenberg, J. E. Herrmann, L. S. Smith, and S. M. Matsui.** 1994. Analysis of astrovirus serotype 1 RNA, identification of the viral RNA-dependent RNA polymerase motif, and expression of a viral structural protein. J. Virol. **68:**77–83.
16. **Madeley, C. R., and B. P. Cosgrove.** 1975. Letter: viruses in infantile gastroenteritis. Lancet **ii:**124.
17. **Marczinke, B., et al.** 1994. The human astrovirus RNA-dependent RNA polymerase coding region is expressed by ribosomal frameshifting. J. Virol. **68:**5588–5595.
18. **Matsui, S. M., and H. B. Greenberg.** 2001. Astroviruses, p. 875–893. *In* B. N. Fields, D. M. Knipe, P. M. Howley, D. E. Griffin, M. A. Martin, R. A. Lamb, B. Roizman, and S. E. Strauss (ed.), Fields virology. Lippincott-Raven, Philadelphia. PA.
19. **Meggio, F., et al.** 1995. Different susceptibility of protein kinases to staurosporine inhibition. Kinetic studies and molecular bases for the resistance of protein kinase CK2. Eur. J. Biochem. **234:**317–322.
20. **Méndez, E., E. Salas-Ocampo, and C. F. Arias.** 2004. Caspases mediate processing of the capsid precursor and cell release of human astroviruses. J. Virol. **78:**8601–8608.
21. **Méndez, E., M. P. Salas-Ocampo, M. E. Munguia, and C. F. Arias.** 2003. Protein products of the open reading frames encoding nonstructural proteins of human astrovirus serotype 8. J. Virol. **77:**11378–11384.
22. **Méndez-Toss, M., P. Romero-Guido, M. E. Munguia, E. Méndez, and C. F.**

Arias. 2000. Molecular analysis of a serotype 8 human astrovirus genome. J. Gen. Virol. **81:**2891–2897.
23. **Monroe, S. S., M. J. Carter, and J. E. Herrmann.** 1995. Family Astroviridae, p. 364–367. *In* F. Murphy, C. Fauquet, and D. Bishop (ed.), Virus taxonomy: classification and nomenclature of viruses. Springer-Verlag, New York, NY.
24. **Monroe, S. S., et al.** 1991. Temporal synthesis of proteins and RNAs during human astrovirus infection of cultured cells. J. Virol. **65:**641–648.
25. **Oh, D., and E. Schreier.** 2001. Molecular characterization of human astroviruses in Germany. Arch. Virol. **146:**443–455.
26. **Pintó, R. M., et al.** 1998. Enhancement of the immunogenicity of a synthetic peptide bearing a VP3 epitope of hepatitis A virus. FEBS Lett. **438:**106–110.
27. **Speroni, S., et al.** 2009. Structural and biochemical analysis of human pathogenic astrovirus serine protease at 2.0 Å resolution. J. Mol. Biol. **387:**1137–1152.
28. **Tamaoki, T., et al.** 1986. Staurosporine, a potent inhibitor of phospholipid/Ca++dependent protein kinase. Biochem. Biophys. Res. Commun. **135:** 397–402.
29. **Willcocks, M. M., N. Ashton, J. B. Kurtz, W. D. Cubitt, and M. J. Carter.** 1994. Cell culture adaptation of astrovirus involves a deletion. J. Virol. **68:**6057–6058.
30. **Willcocks, M. M., A. S. Boxall, and M. J. Carter.** 1999. Processing and intracellular location of human astrovirus non-structural proteins. J. Gen. Virol. **80:**2607–2611.